JOURNAL OF SOLID STATE CHEMISTRY 36, 289–296 (1981)

The Isostructural γ-Sulfur Phase of Selenium–Sulfur, Se_nS_{8-n}

ROBERT A. BOUDREAU AND HELMUT M. HAENDLER*

Department of Chemistry, University of New Hampshire,
Durham, New Hampshire 03824

Received February 6, 1980; in revised form July 21, 1980

Two new selenium–sulfur species, $Se_{1.1}S_{6.9}$ (yellow) and $Se_{3.7}S_{4.3}$ (orange), have been isolated as single crystals, and the corresponding structures have been determined. The space group is $P2/c$, and the parameters are $a = 8.34$ Å, $b = 13.11$ Å, $c = 9.30$ Å, $\beta = 123.9°$ and $a = 8.40$ Å, $b = 13.26$ Å, $c = 9.37$ Å, $\beta = 124.5°$, respectively. They are isostructural with γ-sulfur, having two distinct pairs of eight membered rings in the unit cell. The selenium and sulfur atoms appear scrambled throughout all atomic positions, but are not scrambled equally. When atomic site occupancy data are combined with other data from the literature, a wide compositional continuum of γ-sulfur isostructures is revealed that extends from γ-sulfur to SeS. It appears unlikely that selenium-sulfur crystals exist having the γ-sulfur structure with more than half the atoms as selenium.

Introduction

The development of a complete structural description of covalently bound selenium–sulfur compounds, Se_nS_{8-n}, has been hindered by difficulties in analysis and in isolation of species with discrete compositions (*1–3*). Weiss (*4*) has isolated $Se_{2.9}S_{5.1}$, $Se_{3.3}S_{4.7}$, and $Se_{4.7}S_{3.3}$, and Calvo *et al.* (*5*) have reported on Se_3S_5. The three closely related selenium–sulfur compounds, with the approximate molar ratio of 3 : 5, crystallize as γ-sulfur isostructures (*6*), with scrambled occupancies at all positions. The remaining compound crystallizes in the α-selenium structure. Powder diffraction and mass spectra had shown that mixed crystals might exist over a much broader range of composition. Single crystals of selenium–sulfur, far removed in composition from those previously reported, have been synthesized by a new method, thereby considerably extending the range of observation. Structures have been determined; a pattern for the scrambling of the atomic occupancies over the range Se_0S_8–Se_4S_4 has been established and linked to the stability of these compounds.

Experimental

Preparation and Crystal Growth

$Se_{1.1}S_{6.9}$. Powdered amorphous black selenium (2.0 g) and liquid bromine (2 ml) were vigorously shaken together with 50 ml of methanol (dried with molecular sieves). After 30 min the resulting dark red solution was decanted into a 2-liter distillation flask containing a mixture of 900 ml of freshly dried methanol and 50 ml of methanol that had been saturated (room temperature) with hydrogen sulfide gas. Following reaction, approximately 800 ml of solvent was distilled off, and

---

* To whom correspondence should be addressed.

0022-4596/81/030289-08$02.00/0

the residual yellow solution was filtered hot into a warm flask held in a 2-liter water bath at 65°C. The product, a collection of yellow needle-shaped crystals, grew in the filtrate as the bath cooled.

$Se_{3.7}S_{4.3}$. A mixture of powdered black selenium (1.0 g), liquid bromine (2 ml), and 100 ml of freshly dried methanol was refluxed for 1 hr and then filtered. The solution was gently boiled for 15 min to remove excess bromine, which interferes with crystal formation. Twenty drops of the resulting dark red solution were added, without agitation, to a flask containing 50 ml of methanol saturated with hydrogen sulfide at room temperature, and the mixture was allowed to stand for 24–28 hr. The subsequent reaction produced a slight amount of yellow selenium–sulfur precipitate, which later redissolved, leaving the desired product, a collection of small orange needle-shaped crystals.

Chemical Analysis

The compositions of the selenium–sulfur crystals were determined by X-ray fluorescence (XRF) employing a starch sample pellet matrix (GE XRD3/SPG2 Fluorescence Spectrometer) and by scanning electron microprobe analysis (AMR SEM 1000/EDAX 711 Atom Analyzer). Standards used in conjunction with the XRF determinations contained known weight ratios of pure elements to starch. *Anal* Calcd. for $Se_{1.1}S_{6.9}$: Se, 28.2; S, 71.8. Found: Se, 27.2 ± 0.4; S, 74.0 ± 2.2. Calcd. for $Se_{3.7}S_{4.3}$: Se, 67.9; S, 32.1. Found: Se, 68.0 ± 0.8; S, 30.7 ± 1.1.

Physical Measurements

X-Ray powder patterns for $Se_{1.1}S_{6.9}$ and $Se_{3.7}S_{4.3}$ appeared similar to each other as well as to SeS as listed in the JCPDS file (*7*), but careful measurements revealed increases in lattice spacings proportional to selenium content. The patterns were indexed and are available from the authors, as are structure factor data.

Systematic absences on Weissenberg photographs led first to the nonstandard monoclinic space group $B2/c$ and an orthogonal cell. As with γ-sulfur (*8*) it was possible to transform this to a cell half as large, with extinctions characteristic of $P2/c$ and Pc. Intensity statistics indicated centrosymmetric $P2/c$. Unit cell parameters were determined using zero level Weissenberg and precession photographs. Density measurements were made by flotation in carbon tetrachloride and methylene iodide. Data were collected with multiple film, equi-inclination, integrated Weissenberg photographs using separate crystals mounted on their respective *b* and *c* axes. The intensities were corrected for Lorentz, polarization, and absorption factors prior to using the method of Hamilton *et al.* (*9*) for merging the separate *b* and *c* axial data sets. For $Se_{1.1}S_{6.9}$ and $Se_{3.7}S_{4.3}$, 309 and 568 respective nonzero reflections were recorded, a nonzero reflection being defined as a diffraction spot visible on any film. Crystals used for intensity data collection were approximately 0.07 × 0.02 × 0.30 mm in size. Each absorption correction was integrated over 512 points. With $Se_{3.7}S_{4.3}$, the transmission coefficient, T, in the expression, $I_{\text{corr}} = I_{\text{obsd}}/T$, ranged from 0.219 to 0.552 for rotation about *c* and 0.025 to 0.401 for rotation about *b*. The scattering factors used were those of Hanson *et al.* (*10*). The crystal data are summarized in Table I.

Structure Determination and Refinement

Similar structural characteristics indicated that the compounds were probably isostructural with each other as well as with γ-sulfur. To confirm this, trial structures starting with the atomic positions of γ-sulfur were refined for both $Se_{3.7}S_{4.3}$ and $Se_{1.1}S_{6.9}$. The refinement employed a pseudo-sulfur structural model comprised

TABLE I

CRYSTAL DATA[a]

	γ-sulfur	$Se_{1.1}S_{6.9}$	$Se_{3.7}S_{4.3}$
a	8.44 Å	8.34(9) Å	8.40(8) Å
b	13.02 Å	13.11(4) Å	13.26(10) Å
c	9.36 Å	9.30(6) Å	9.37(2) Å
β	125.0°	123.9(9)°	124.5(8)°
V	843.0 Å^3	844.3 Å^3	860.1 Å^3
D_m	2.19 g cm^{-3}	2.10 g cm^{-3}	3.32 g cm^{-3}
D_x	2.08 g cm^{-3}	2.42 g cm^{-3}	3.26 g cm^{-3}
Z	4	4	4
μ(Cu$K\alpha$)	179.9 cm^{-1}	188.4 cm^{-1}	257.1 cm^{-1}

[a] Space group $P2/c$; hkl: all orders; $h0l$: $l = 2n$.

totally of sulfur atoms but having variable occupancy at each atomic site. Parameters were determined by a least-squares method with a block diagonal approximation. R-values for the pseudo-sulfur approximations, with anisotropic temperature factors, were 0.080 and 0.097, respectively, for $Se_{3.7}S_{4.3}$ and $Se_{1.1}S_{6.9}$. The sulfur occupancies obtained were generally greater than 1.0, reflecting the increased electron densities owing to the selenium presence. The parameters are summarized in Tables II and III.

The actual selenium and sulfur occupancies at each atomic site were determined by a system of equations incorporating the relative electron densities expressed by the pseudo-occupancies, as well as the analyzed composition of the crystals:

$$N_{mS} = S_m + K\mathrm{Se}_m \qquad (1)$$

$$S_m + \mathrm{Se}_m = 1 \qquad (2)$$

$$\sum_{m=1}^{8} \mathrm{Se}_m = X_{\mathrm{Se}}. \qquad (3)$$

TABLE II

POSITIONAL AND THERMAL PARAMETERS FOR THE PSEUDO-SULFUR STRUCTURE $Se_{3.7}S_{4.3}$

Positional parameters

Atom	x	y	z	N_{mS}[a]
S(1)	0.6561(8)	0.3406(4)	0.3269(8)	1.368(27)
S(2)	0.8139(9)	0.5819(6)	0.4722(9)	0.983(25)
S(3)	0.7512(8)	0.4444(5)	0.5427(8)	1.164(25)
S(4)	0.5844(10)	0.6781(6)	0.3868(9)	0.991(25)
S(5)	0.0807(10)	0.7962(5)	0.1941(9)	1.133(27)
S(6)	0.2449(10)	1.0372(6)	0.2125(9)	1.131(27)
S(7)	0.3167(9)	0.8958(6)	0.3538(9)	1.106(26)
S(8)	0.1496(13)	1.1328(5)	0.3322(10)	1.098(28)

Anisotropic thermal parameters (× 10^4 Å^2)[b,c]

Atom	U_{11}	U_{22}	U_{33}	U_{12}	U_{13}	U_{23}
S(1)	653(48)	456(44)	592(50)	48(28)	389(38)	269(37)
S(2)	250(42)	560(61)	343(52)	44(35)	242(37)	−24(41)
S(3)	442(45)	548(50)	225(41)	116(29)	254(32)	61(37)
S(4)	542(55)	416(55)	434(60)	−71(35)	421(47)	−65(42)
S(5)	703(58)	411(51)	640(61)	−95(34)	525(47)	15(40)
S(6)	688(59)	726(65)	572(62)	−225(36)	579(49)	−424(45)
S(7)	266(42)	870(79)	498(56)	−149(41)	189(38)	115(46)
S(8)	1138(75)	435(56)	567(62)	−198(38)	567(54)	−442(53)

[a] Site occupation factor.

[b] The anisotropic thermal parameters are defined as: $f = f_0\exp(-2\pi^2(U_{11}h^2a^{*2} + 2U_{12}hka^*b^* + \ldots\ldots))$.

[c] Estimated standard deviations are given in parentheses.

TABLE III

POSITIONAL AND THERMAL PARAMETERS FOR THE PSEUDO-SULFUR STRUCTURE $Se_{1.1}S_{6.9}$

Positional parameters

Atom	x	y	z	N_{mS}[a]
S(1)	0.6540(16)	0.3436(9)	0.3246(16)	1.096(46)
S(2)	0.8134(17)	0.5801(10)	0.4641(16)	0.967(45)
S(3)	0.7457(17)	0.4454(10)	0.5380(17)	1.038(44)
S(4)	0.5823(20)	0.6759(10)	0.3872(17)	0.935(45)
S(5)	0.0805(18)	0.7991(9)	0.1964(16)	1.201(47)
S(6)	0.2404(21)	1.0334(10)	0.2157(18)	1.153(49)
S(7)	0.3105(18)	0.8951(11)	0.3513(18)	1.163(51)
S(8)	0.1495(22)	1.1274(10)	0.3281(18)	1.190(52)

Anisotropic thermal parameters ($\times 10^4$ Å^2)[b,c]

Atom	U_{11}	U_{22}	U_{33}	U_{12}	U_{13}	U_{23}
S(1)	284(100)	359(99)	368(115)	183(66)	586(136)	363(70)
S(2)	292(101)	508(118)	27(116)	67(73)	540(144)	−107(77)
S(3)	247(89)	605(110)	69(112)	200(71)	358(123)	52(77)
S(4)	623(125)	249(102)	−56(114)	−129(68)	585(157)	−28(73)
S(5)	607(102)	419(98)	431(117)	−141(66)	739(132)	21(69)
S(6)	751(127)	712(133)	190(125)	−124(69)	578(153)	−387(86)
S(7)	301(95)	701(122)	542(125)	−25(81)	240(136)	−0(80)
S(8)	935(130)	605(118)	490(125)	−151(76)	780(160)	−301(88)

[a] Site occupation factor.

[b] The anisotropic thermal parameters are defined as: $f = f_0 \exp(-2\pi^2(U_{11}h^2a^{*2} + 2U_{12}hka^*b^* + \ldots\ldots))$.

[c] Estimated standard deviations are given in parentheses.

Equation (1) approximates N_{mS}, the refined pseudo-occupancy of sulfur at position m in the cell, by a linear combination of the real occupancies for sulfur and selenium, S_m and Se_m. It utilizes the approximate proportionality of the selenium and sulfur scattering factors at the appropriate diffraction angles. Equation (2) assumes that each asymmetric position, m, is occupied by either one element or the other and is never vacant. Equation (3) assumes that the total occupancy, $\sum_{m=1}^{8} Se_m$, of selenium in the asymmetric unit is the same as the measured selenium mole fraction, X_{Se}, for the crystals in bulk. After the actual occupancies, S_m and Se_m, were determined for $Se_{3.7}S_{4.3}$, using the pseudo-sulfur approximation, the method was checked by recalculation with a corresponding pseudo-selenium approximation. The derived actual occupancies were in good agreement with those obtained from the pseudo-sulfur approximation, and the pseudo-selenium positional parameters refined to within 0.001 Å of those obtained for pseudo-sulfur. The calculated occupancies and their propagated errors are shown in Table IV.

Discussion

The symmetry elements and contents of the unit cell, representing either $Se_{3.7}S_{4.3}$ or $Se_{1.1}S_{6.9}$, are illustrated in Fig. 1. Two distinct types of rings exist, each centered on

TABLE IV

SELENIUM FRACTIONAL OCCUPANCIES FOR $Se_{3.7}S_{4.3}$ AND $Se_{1.1}S_{6.9}$ DERIVED FROM THE PSEUDO-Se AND S STRUCTURES

		$Se_{3.7}S_{4.3}$		
		Pseudo-S based	Pseudo-Se based	Average
Ring 1	Se(1)	1.00(31)	0.72(3)	0.86(17)
	Se(2)	0.00(9)	0.31(5)	0.16(7)
	Se(3)	0.61(16)	0.55(3)	0.58(10)
	Se(4)	0.00(9)	0.32(7)	0.16(8)
Ring 2	Se(5)	0.49(14)	0.47(4)	0.48(9)
	Se(6)	0.48(14)	0.47(4)	0.48(9)
	Se(7)	0.39(13)	0.45(4)	0.42(9)
	Se(8)	0.36(13)	0.45(4)	0.41(9)
		$Se_{1.1}S_{6.9}$		
		Pseudo-S based		
Ring 1	Se(1)	0.12(9)		
	Se(2)	0.00(4)		
	Se(3)	0.06(6)		
	Se(4)	0.00(4)		
Ring 2	Se(5)	0.26(16)		
	Se(6)	0.20(13)		
	Se(7)	0.21(13)		
	Se(8)	0.24(15)		

twofold rotation axes. One pair of rings, whose twofold rotation axes lie within the cell, are classified as belonging to type 1 (R1), while the remaining rings, having twofold axes which intersect the *c* axis, are classified as ring type 2 (R2).

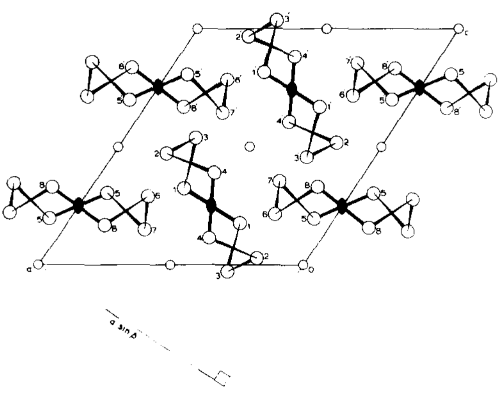

FIG. 1. Projection of the unit cell along the *b* axis.

The intramolecular bond distances and angles are listed in Table V. These, with the occupancy factors, illustrate the construction of the molecular crowns and reflect further differences between R1 and R2. Ring R2 contains an even distribution of occupancies and bond lengths, while R1 is polarized in the *b* direction, having much of its selenium content at one end. For $Se_{3.7}S_{4.3}$ and $Se_{1.1}S_{6.9}$, average bond distances for the more evenly distributed R2 are 2.130 and 2.064 Å, respectively, compared to 2.044 Å for γ-sulfur (*6*) and 2.34 Å for monoclinic α- or β-selenium (*11*). Ring R1 atomic positions 1 and 3, with the highest selenium occupancy, bond approximately 0.1 Å farther apart than positions 2 and 4 in both selenium–sulfur compounds.

The intermolecular distances remain essentially the same for the selenium–sulfur compounds as they do for γ-sulfur. The

TABLE V

BOND DISTANCES AND ANGLES (BASED ON PSEUDO-SULFUR)

Intramolecular bond distances and angles

	$Se_{3.7}S_{4.6}$	$Se_{1.1}S_{6.9}$
S(1)–S(3)	2.189(9) Å	2.145(18) Å
S(2)–S(3)	2.106(10)	2.083(21)
S(2)–S(4)	2.059(12)	2.065(23)
S(5)–S(7)	2.132(11)	2.063(21)
S(6)–S(7)	2.173(11)	2.098(20)
S(6)–S(8)	2.127(13)	2.017(24)
S(1)–S(1)	2.162(11)	2.134(21)
S(4)–S(4)	2.113(11)	2.118(19)
S(5)–S(5)	2.133(13)	2.069(24)
S(8)–S(8)	2.074(15)	2.073(26)
S(1)–S(1)–S(3)	106.6(4)°	106.3(8)°
S(1)–S(3)–S(2)	106.2(4)	105.1(8)
S(3)–S(2)–S(4)	108.2(4)	104.2(8)
S(2)–S(4)–S(4)	107.9(5)	105.6(9)
S(5)–S(5)–S(7)	104.6(4)	105.3(8)
S(5)–S(7)–S(6)	106.2(4)	105.9(9)
S(7)–S(6)–S(8)	104.6(5)	105.5(9)
S(6)–S(8)–S(8)	105.6(5)	106.8(9)

Intermolecular bond distances[a,b]

Atomic positional pairs[c]	$Se_{3.7}S_{4.3}$	$Se_{1.1}S_{6.9}$	γ-Sulfur
(1)–(5)	3.74(1) Å	3.80(2) Å	3.81 Å
(3)–(4′)	3.62(1)	3.55(2)	3.65
(2)–(2′)	3.59(1)	3.50(2)	3.58
(5)–(2)	3.59(1)	3.57(2)	3.62
(4)–(8′)	3.40(1)	3.47(2)	3.45
(7)–(8′)	3.74(1)	3.78(2)	3.80
(7)–(6′)	3.84(1)	3.86(2)	3.75
(5)–(4)	3.66(1)	3.69(2)	3.69
(5)–(3′)	3.78(1)	3.81(2)	3.75

[a] Shortest atomic bond distances are tabulated.

[b] Refer to Fig. 1 for prime notation.

[c] Atomic position numbering scheme refers to sulfur or selenium distances.

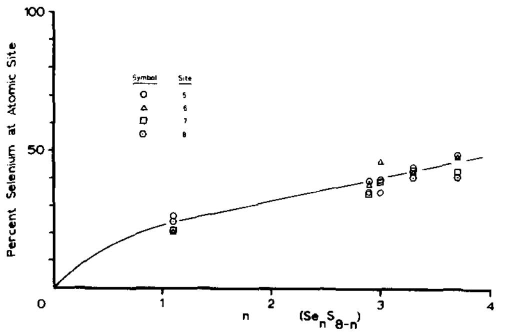

FIG. 2. Site occupancy for ring 2.

variation in unit cell size, as selenium composition is increased, apparently results mainly from the intramolecular covalent forces, and accounts for the powder pattern trends found between different selenium–sulfur compositions, isostructural with γ-sulfur.

Figures 2 and 3 illustrate the continuous variation of selenium occupancy found throughout the γ-sulfur phase of selenium–sulfur, including data reported elsewhere (*4*, *5*).† It will be noted that the new data extend the range of composition at both ends. As selenium composition is increased, rings R1 and R2 incorporate selenium differently. With ring R2, selenium is equally incorporated at each atomic site, approximating the fractional composition of the compound as a whole. In contrast, ring R1 contains several sites which incorporate selenium differently. The selenium composition of site 1 rises quickly, ap-

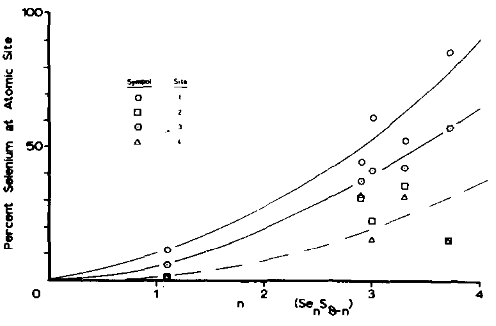

FIG. 3. Site occupancy for ring 1.

---

† In Table 3 of reference (*4*) the coordinates of positions 7 and 8 have been reversed. Not all distances in Fig. 1 are in agreement with the parameters listed.

proaching the 100% selenium limit at the point at which the selenium–sulfur ratio is 1 : 1. At site 3, selenium incorporation is lower but follows a similar trend. Sites 2 and 4 display the least selenium incorporation and the weakest trend. Throughout the γ-sulfur phase, ring R1 polarizes its ever increasing selenium content along the *b* direction.

A model of ordered arrangements, for example a mixed crystal of Se_4S_4 and Se_2S_6 (average Se_3S_5) or of Se_2S_6 and S_8 (average SeS_7), is not likely for these compounds. Mass spectral analysis of $Se_{3.7}S_{4.3}$ confirmed earlier results by Cooper and Culka (*3*) that a wide distribution of molecules, possessing different combinations of selenium and sulfur atoms, is present. Fourier maps show a continuous range of electron density throughout the molecular rings, with the higher electron density found at sites having the most selenium occupancy.

It appears unlikely that the continuum of selenium–sulfur isostructures extends to compositions with more than half the atoms as selenium, confirming an earlier powder diffraction study (*2*). The selenium occupancy at site 1 of ring R1 reaches the physical limit of 100% when *n* is 4, and there may be stability problems related to electronegativities (*3*), which discourage the placement of many adjacent selenium atoms, a condition existing with high selenium composition. Presently, the only known selenium–sulfur structure having a composition with *n* greater than 4 has the α-selenium structure, posing the possibility of a second isostructural phase conforming to the structure of its predominant element.

The similar characteristics of the selenium and sulfur atoms present a special case of nonstoichiometry. Nonstoichiometric compounds (*12*) which exhibit isostructural phases of varying composition usually do not exhibit the covalent molecular composition which is characteristic of selenium–sulfur, but rather are interstitial defect structures or solid solutions (*13*). The range of stoichiometry for the γ-sulfur isostructures is quite unusual since most nonstoichiometric compounds cannot suppress the structural strain imposed by a wide variation in composition.

Acknowledgments

We are grateful to Professor Frederick Hochgraf of the Department of Mechanical Engineering and to Dr. David Swift of the Center for Institutional and Industrial Development, University of New Hampshire, for assistance with microscopy and X-ray fluorescence. The program WABS (*14*) was used for the absorption correction. Other computations were made using the National Research Council of Canada Crystallographic programs (*15*).

References

1. J. E. Fergusson, G. M. Pratt, G. A. Rodley, and C. J. Wilkins, *J. Inorg. Nucl. Chem.* **24**, 157 (1962).

2. C. R. Allwood and P. E. Fielding, *Aust. J. Chem.* **22**, 2301 (1968).

3. R. Cooper and J. V. Culka, *J. Inorg. Nucl. Chem.* **29**, 1217 (1967).

4. J. Weiss, *Z. Anorg. Allg. Chem.* **435**, 113 (1977).

5. C. Calvo, R. J. Gillespie, J. E. Vekris, and H. N. Ng, *Acta Crystallogr.* **B34**, 911 (1978).

6. Y. Watanabe, *Acta Crystallogr.* **B30**, 1396 (1974).

7. "Powder Diffraction File," Joint Committee on Powder Diffraction Standards, Swarthmore, Pa. (1978).

8. J. Donahue and B. Meyer, *in* "Elemental Sulfur" (B. Meyer, Ed.), p. 31. Interscience, New York (1965).

9. W. C. Hamilton, J. S. Rollett, and R. A. Sparks, *Acta Crystallogr.* **18**, 129 (1965).

10. H. P. Hanson, F. Herman, J. D. Lee, and S. Skillman, *Acta Crystallogr.* **17**, 1040 (1964).

11. K. W. Bagnall, "The Chemistry of Selenium, Tellurium and Polonium," p. 34. Elsevier, New York (1966).

12. A. D. Wadsley *in* "Non-Stoichiometric Compounds" (L. Mandelcorn, Ed.). Academic Press, New York (1964).

13. A. F. WELLS, "Structural Inorganic Chemistry", 3rd ed., p. 167. Oxford University Press, Oxford, (1962).

14. J. A. IBERS, Northwestern University, Evanston, Illinois (1968 version).

15. F. R. AHMED, National Research Council Crystallographic Series, National Research Council, Ottawa, Canada.